24th COBEM - 2017

24th ABCM International Congress of Mechanical Engineering
December 3-8, 2017, Curitiba, PR, Brazil

COBEM-2017-2431
RECURSIVE METHODOLOGY APPLIED TO DETERMINATION OF SEMI-ANALYTICAL SOLUTION OF ANISOTROPIC THICK PLATES IN LINEAR BENDING

Tales de Vargas Lisbôa
Rogério José Marczak
Department of Mechanical Engineering - Federal University of Rio Grande do Sul
taleslisboa@daad-alumni.de, rato@mecanica.ufrgs.br

Abstract. *The objective of this paper is to analyse a recursive methodology so as to determine semi-analytical solution of anisotropic thick plates. This methodology is based on Adomian Decomposition and pb-2 Rayleigh-Ritz methods. The first one can be defined by three main characteristics: the decomposition of the differential/matrix operator; the expansion of the problem's solution in an infinite series and the determination of each term by a recursive procedure that relates a specific term of the expansion to the previous terms as well as to the decomposed parts of the operator. The second method approximates the solution's space by weighted kinematically admissible interpolation functions. By the minimization of the total potential functional, each function's weight is defined, resulting in a global response of the problem. Along with Adomian Decomposition Method, the solution expansion is related to an infinite sum of weighting vector of Rayleigh-Ritz Method. The convergence of the recursive methodology is presented and numeric results are provided and good agreement is achieved when compared to solutions found in the literature.*

Keywords: *Adomian Decomposition Method, Anisotropic thick plates, Rayleigh-Ritz Method, Semi-analytic solutions*

1. INTRODUCTION

The paper's objective is to present a methodology which determines the anisotropic thick plates response in a recursive fashion. Mindlin's Plate Theory (Mindlin (1951); Reddy (2007)) is considered along with *pb-2* Rayleigh-Ritz Method (Bhat (1985); Liew and Wang (1993)) to solve its equilibrium equations. A proposed scheme to additively decompose the constitutive tensor is shown, which is utilised to extract an isotropic part from an anisotropic tensor that constitutes the plate. By Adomian Decomposition Method (Adomian (1994)), this isotropic solution is recursively enhanced by the anisotropic influence of the domain.

Mindlin's Plate Theory (MPT) describes more precisely the structural response of thick plates when compared to the Classical Plate Theory, given the consideration of the transverse shear in the deformation. This structural theory is essentially the counterpart of Timoshenko's beam theory in plates. Given a discordance between the theoretical shear stress (parabolic form) and the obtained by the aforementioned theory (constant form in most of the cases), the transverse shear is weighted by a correction factor, which can be obtained, for example, by equivalencing the work produced in both cases (Reddy (2007); Jemielita (2002)).

Hooke's Law is used to construct the stress-strain relationship. Some inner connections among the elastic constants are developed depending on the symmetry of the crystal. The least symmetric material that could be evaluate in plates is the monoclinic symmetry (Alternbach (1998)), regarding the hierarchic tree (Cowin and Mehrabadi (1995); Chadwick *et al.* (2001); Ting (2003)) based on crystal system. The hierarchy concept concerns to connections among the symmetric groups and their reflexive planes. Regarding these relations, an additive decomposition which extracts an specific (higher) symmetry from another (lower one) can be derived: Tu (Tu (1968)) and Browayes & Chevrot (Browaeys and Chevrot (2004)) have developed two similar additive decompositions for three-dimensional constitutive tensors. The original tensor is then reconstructed by adding the remainder term to the extracted one. This tool was normally used in verifying how close an anisotropic tensor is to an isotropic one. In this paper, it will be used to decompose the differential operator.

Rayleigh-Ritz Method (RRM) (Bhat (1985); Liew and Wang (1993)) is used to solve the governing equations of Mindlin Plate Theory. It utilises a superposition of linearly independent kinematically admissible functions to interpolate the problem's degrees-of-freedom. By the minimisation of the Total Potential Energy Functional, constructed adding the strain energy and the external potential, the interpolation functions' weighting constants can be determined. Through the adopted modification, namely *pb-2*, the requirement of the functions being kinematically admissible is contoured by inserting zeros in the entire basis (Bhat (1985)), at the plate's boundary, enforcing the problems' boundary conditions. By

using this method, Kitipornchai et al. (Kitipornchai *et al.* (1994)) have studied the free vibration behaviour of isotropic thick trapezoidal plates with several boundary conditions sets while Singh and Elaghabash (Singh and Elaghabash (2003)) have analysed finite displacement of isotropic plates by considering the von Kármán hypothesis. Bhat (Bhat (1985)) and Liew & Wang (Liew and Wang (1993)) have utilised the method in order to obtain global static solutions for thin isotropic plates.

Adomian Decomposition Method (ADM) (Adomian (1994)) is used to determine recursively the anisotropic behaviour of thick plates. The method has three main characteristics: decomposition of the differential/matrix operator; expansion of the solution into an infinite series; and the determination of each solution term in a recursive manner. In truncating the series in a specific term, it is possible to construct a laborious solution by enhancing a simpler one with more complex terms. The methodology has been applied to determine the static behaviour of laminated (Lisbôa and Marczak (2017)) thin plates. Biazar el al. (Biazar *et al.* (2004)) and Babolian & Biazar (Babolian and Biazar (2002)) have demonstrated that the decomposition can be applied to ordinary non-linear equations.

The objective of this paper is to evaluate ADM applied to anisotropic thick plates. Firstly, the governing equations of MPT are demonstrated and both strain energy and external potential are presented. Then, the additive decomposition is proposed and the hierarchic tree is modified to the reduced constitutive tensor. The *pb-2* RRM is applied to the governing equations and the functional and its first variation are defined in terms of the weighting constants. The matrix operator is decomposed by the aforementioned constitutive decomposition. The ADM recursive procedure is then assembled, whose first step concerns an isotropic solution of the problems while the subsequent ones are anisotropic enhancements. Numeric results are produced and compared to those found in the literature. The recursive procedure convergence is also shown.

This report is followed by five sections. In the following section the governing equation of anisotropic thick plates are presented as well as the constitutive hierarchy and the projections, used in the additive constitutive decomposition. Furthermore, the *pb-2* RRM is presented already applied to the thick plate governing equations. Then, ADM is introduced and applied to the linear system developed by RRM and it is followed by a discussion on the convergence of the methodology, in the third section. After, numeric results using the methodology are developed. The obtained solutions are posed and compared to those found in the literature along with tables containing numeric results for cases of study. In the last section, conclusions are presented and discussed.

In the report, both matrix and index notation are used. In the first, small-caps and high-caps bold letters denote 1st order and 2nd or higher order tensors, respectively, while non-bold letters describe scalars. All vectors are defined as column-vector. In Index notation, Roman integer small-caps and high-caps indices goes from 1 to 3 and 1 to N (which is always provided), respectively, while on Greek integer indices, the range of variation is 1 to 2. Repeated indices denote summation unless otherwise expressed and comma corresponds to differentiations over the following indices.

2. MODELLING

2.1 Mindlin's Plate Theory

The displacement field of moderately thick plates described by MPT is written as (Reddy (2007))

$$\begin{aligned} U_1\left(x_1,x_2,x_3\right) &\doteq -x_3\theta_1\left(x_1,x_2\right),\\ U_2\left(x_1,x_2,x_3\right) &\doteq -x_3\theta_2\left(x_1,x_2\right),\\ U_3\left(x_1,x_2\right) &\doteq u_3\left(x_1,x_2\right), \end{aligned}$$

where U_k denote the three-dimensional orthogonal displacement, θ_α describe the rotation in relation of the mid-surface in the α direction and u_3 corresponds to the transverse displacement while x_k represent the Cartesian coordinates.

The strain vector, $\boldsymbol{\epsilon}$, is determined by the linear kinematic relation as (Singh and Elaghabash (2003))

$$\boldsymbol{\epsilon} = \mathbf{H}\boldsymbol{\partial}\mathbf{d}, \tag{1}$$

where

$$\boldsymbol{\epsilon} = \begin{Bmatrix} \epsilon_{11}\\ \epsilon_{22}\\ \epsilon_{23}\\ \epsilon_{13}\\ \epsilon_{12} \end{Bmatrix}, \qquad \mathbf{H} = \begin{bmatrix} 0 & 0 & -x_3 & 0 & 0\\ 0 & 0 & 0 & -x_3 & 0\\ 1 & 0 & 0 & 0 & 0\\ 0 & 1 & 0 & 0 & 0\\ 0 & 0 & 0 & 0 & -x_3 \end{bmatrix}, \qquad \boldsymbol{\partial} = \begin{bmatrix} \dfrac{\partial}{\partial x_2} & 0 & -1\\ \dfrac{\partial}{\partial x_1} & -1 & 0\\ 0 & \dfrac{\partial}{\partial x_1} & 0\\ 0 & 0 & \dfrac{\partial}{\partial x_2}\\ 0 & \dfrac{\partial}{\partial x_2} & \dfrac{\partial}{\partial x_2} \end{bmatrix},$$

Table 1. Essential and natural boundary conditions

• Clamped Edge :	$\overline{u}_3 = 0$ on $\partial\Lambda_u$,	$\overline{\theta}_{\mathbf{n}} = 0$ on $\partial\Lambda_u$,	$\overline{\theta}_{\mathbf{t}} = 0$ on $\partial\Lambda_u$,
• Simply-Suported Edge :	$\overline{u}_3 = 0$ on ∂, Λ_u	$\overline{\theta}_{\mathbf{t}} = 0$ on $\partial\Lambda_u$,	$\overline{M}_{\mathbf{nn}} = 0$ on $\partial\Lambda_n$,
• Free Edge :	$\overline{S}_{\mathbf{n}3} = 0$ on $\partial\Lambda_n$,	$\overline{M}_{\mathbf{nn}} = 0$ on $\partial\Lambda_n$,	$\overline{M}_{\mathbf{nt}} = 0$ on $\partial\Lambda_n$.

and

$$\mathbf{d} = \begin{Bmatrix} u_3 & \theta_1 & \theta_2 \end{Bmatrix}^{\mathrm{T}}.$$

By the Generalised Hooke's law, the stress vector is written as

$$\boldsymbol{\sigma} = \mathbf{Q}\boldsymbol{\epsilon}, \qquad \mathbf{Q} = \mathbf{R}^{\mathrm{T}}\hat{\mathbf{C}}\mathbf{R}, \tag{2}$$

where $\mathbf{Q}$, $\mathbf{R}$ and $\hat{\mathbf{C}}$ are the transformed constitutive tensor, the transformation matrix and the reduced constitutive tensor, respectively. In its principal directions, $\hat{\mathbf{C}}$ can be defined as

$$\hat{\mathbf{C}} = \begin{bmatrix} \hat{C}_{11} & \hat{C}_{12} & 0 & 0 & \hat{C}_{16} \\ & \hat{C}_{22} & 0 & 0 & \hat{C}_{26} \\ & & \kappa_{11}\hat{C}_{44} & \kappa_{12}\hat{C}_{45} & 0 \\ & & & \kappa_{22}\hat{C}_{55} & 0 \\ sym & & & & \hat{C}_{66} \end{bmatrix}, \tag{3}$$

where

$$\hat{\mathbf{C}} \doteq C_{IJ}^{\mathrm{RED}} = C_{IJ} - \frac{1}{C_{33}} C_{I3} C_{3J},$$

in which $\mathbf{C}$, $\mathbf{C}^{\mathrm{RED}}$ and $\hat{\mathbf{C}}$ denote the 6×6 anisotropic constitutive tensor, the 6×6 reduced anisotropic constitutive tensor with the 3rd line/column filled with zeros, and the 5×5 reduced anisotropic constitutive tensor, respectively. $\hat{\mathbf{C}}$ is assembled by excluding the 3rd line/column from $\mathbf{C}^{\mathrm{RED}}$. The correction on the shear stress, $\kappa_{\alpha\beta}$, for anisotropic homogeneous plates are set as $\kappa_{\alpha\beta} = \frac{5}{6}$ Reddy (2007); Jemielita (2002). The constitutive tensor of Eq. (3) is related to a monoclinic symmetry, with 9 independent constants.

The bending (M_{11}, M_{22}) and twisting (M_{12}) moments as well as the transverse shear stress (S_{13}, S_{23}) are derived as (Reddy (2007, 2004))

$$\mathbf{M} = \mathbf{D}\boldsymbol{\varepsilon}^{\mathrm{B}}, \qquad \mathbf{D} = \frac{h^3}{12}\hat{\mathbf{C}}^{\mathrm{B}}, \qquad \boldsymbol{\varepsilon}^{\mathrm{B}} = \begin{Bmatrix} \theta_{1,1} & \theta_{2,2} & \theta_{1,2} + \theta_{2,1} \end{Bmatrix}^{\mathrm{T}},$$
$$\mathbf{S} = \mathbf{A}\boldsymbol{\varepsilon}^{\mathrm{S}}, \qquad \mathbf{A} = h\hat{\mathbf{C}}^{\mathrm{S}}, \qquad \boldsymbol{\varepsilon}^{\mathrm{S}} = \begin{Bmatrix} u_{3,2} - \theta_2 & u_{3,1} - \theta_1 \end{Bmatrix}^{\mathrm{T}},$$

where $\mathbf{D}$ and $\mathbf{A}$ are the bending and extensional stiffness matrix, respectively, and

$$\hat{\mathbf{C}}^{\mathrm{B}} = \begin{bmatrix} \hat{C}_{11} & \hat{C}_{12} & \hat{C}_{16} \\ & \hat{C}_{22} & \hat{C}_{26} \\ sym & & \hat{C}_{66} \end{bmatrix}, \qquad \hat{\mathbf{C}}^{\mathrm{S}} = \begin{bmatrix} \kappa_{11}\hat{C}_{44} & \kappa_{12}\hat{C}_{45} \\ sym & \kappa_{22}\hat{C}_{55} \end{bmatrix},$$

and

$$\mathbf{M} = \begin{Bmatrix} M_{11} & M_{22} & M_{12} \end{Bmatrix}^{\mathrm{T}}, \qquad \mathbf{S} = \begin{Bmatrix} S_{23} & S_{13} \end{Bmatrix}^{\mathrm{T}}.$$

The equilibrium in terms of the equivalent stress are then defined as (Reddy (2007))

$$M_{\alpha\beta,\alpha\beta} + q_3 = 0,$$
$$S_{\alpha 3,\alpha} + q_3 = 0,$$

where q_3 refers to the transverse loading. Their boundary conditions are written as listed in Tab. 1 (Reddy (2004)) where $\partial\Lambda_e \cup \partial\Lambda_n = \partial\Lambda$, $\partial\Lambda_e \cap \partial\Lambda_n = \emptyset$, $\partial\Lambda_e$ and $\partial\Lambda_n$ are the boundary parts in which the essential and natural boundary

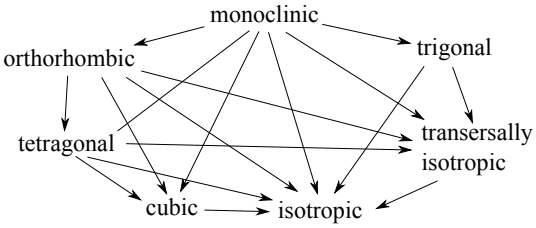

Figure 1. Constitutive Hierarchy

conditions are known, respectively and Λ represents the reference surface. $\mathbf{n}$ and $\mathbf{t}$ define the normal and tangential vectors at the boundary. $\bar{(\cdot)}$ denotes an imposition on the function at the boundary.

With the strains (Eq. (1)) and stress (Eq. (2)) defined, one can determine the plate's strain energy, $W_{\rm int}$, as

$$W_{\rm int} = \frac{1}{2}\int_{\Omega} \boldsymbol{\sigma}^{\rm T}\boldsymbol{\epsilon}\ {\rm d}\Omega = \frac{1}{2}\int_{\Omega} \mathbf{d}^{\rm T}\boldsymbol{\partial}^{\rm T}\mathbf{H}^{\rm T}\hat{\mathbf{C}}\mathbf{H}\boldsymbol{\partial}\mathbf{d}\ {\rm d}\Omega = \frac{1}{2}\int_{\Lambda} \mathbf{d}^{\rm T}\boldsymbol{\partial}^{\rm T}\mathbf{T}\boldsymbol{\partial}\mathbf{d}\ {\rm d}\Lambda, \tag{4}$$

where the stiffness matrix $\mathbf{T}$ is characterised by

$$\mathbf{T} = \int_{-h/2}^{h/2} \mathbf{H}^{\rm T}\hat{\mathbf{C}}\mathbf{H}\ {\rm d}x_3, \tag{5}$$

The external potential, $W_{\rm ext}$, is written as following

$$W_{\rm ext} = -\int_{\Lambda} \mathbf{q}^{\rm T}\mathbf{d}\ d\Lambda, \tag{6}$$

in which

$$\mathbf{q} = \begin{Bmatrix} q_3 & 0 & 0 \end{Bmatrix}^{\rm T}.$$

2.2 Additive Decomposition and Hierarchy

Cowin and Mehrabadi (Cowin and Mehrabadi (1995)), Chadwick et al. (Chadwick *et al.* (2001)) and Ting (Ting (2003)) have developed the concept of constitutive hierarchy. Essentially, when the group of symmetric planes that constitutes a symmetry is a subgroup of another one a hierarchy relation is constructed. Another way to observe such preposition is when one inserts symmetric planes into a symmetric set to develop another symmetry, a hierarchic relationship between both is created.

It is worth noting that depending on the structural theory, the hierarchy changes given the reductions in the constitutive tensor (Lisbôa *et al.* (2017)). Nevertheless, in using MPT, the symmetries as well as the hierarchy are similar to the three-dimensional elasticity (Chadwick *et al.* (2001); Ting (2003)) (excluding the triclinic symmetry (Alternbach (1998))), as one observes in Fig. 1. However, the function of the constitutive hierarchy herein is to guide the decomposition procedure. For sake of simplicity, only the required projections (minimum number) are shown in Fig. 2.

The projections (Fig. 2) concept follows the procedures of Browayes and Chevrot (Browaeys and Chevrot (2004)), being nevertheless structurally different. The idea herein is to develop a mathematical tool to extract a constitutive tensor with a specific symmetry respecting its inner relationships only. The projections are matrix operators applied to vectors that represent the constitutive tensor and they extract a lower symmetry from a higher one as

$$\mathbf{y}^{(L)} = \mathbf{P}^{(L)}_{(H)}\mathbf{y}^{(H)},$$

where $\mathbf{y}^{(X)}$, $X = \{L \quad H\}$ is the vectorised form of the reduced constitutive tensor defined by

$$\mathbf{y}^{(\rm ful)} = {\rm vech}\left(\hat{\mathbf{C}}\right) = \Big\{\hat{C}_{11} \quad \hat{C}_{12} \quad \hat{C}_{14} \quad \hat{C}_{15} \quad \hat{C}_{16} \quad \hat{C}_{22} \quad \hat{C}_{24} \quad \hat{C}_{25} \quad \hat{C}_{26} \quad \hat{C}_{44} \quad \hat{C}_{45} \quad \hat{C}_{46} \quad \hat{C}_{55} \quad \hat{C}_{56} \quad \hat{C}_{66}\Big\}^{\rm T},$$

which only the independent constants are taken into account and the superscript $({\rm ful})$ denotes a full populated reduced constitutive tensor. The scripts (H) and (L) denote higher and lower, respectively, in terms on the hierarchic tree (Fig. 1). Moreover, differently from ref. (Browaeys and Chevrot (2004)) the ${\rm vech}$ function (half-vectorisation) is used and even for the decomposition in lower symmetries, the 15×15 full projector is considered due to some properties that are presented next.

These main properties arise in the projections $\mathbf{P}^{({\rm L})}_{({\rm H})}$, given their mathematical meaning: basically, these operations insert planes into a symmetric set to develop another one. Therefore, they present characteristics as

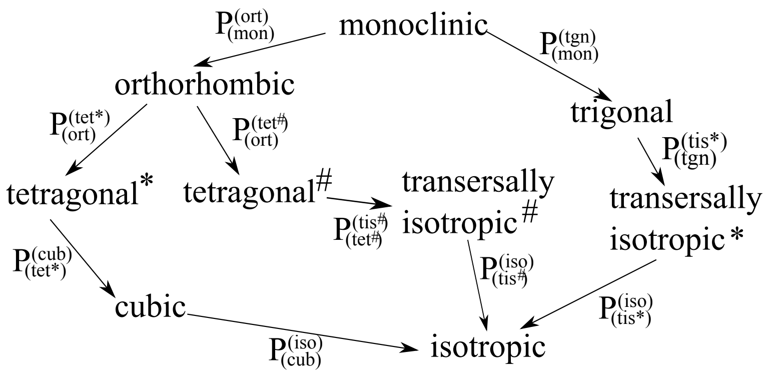

Figure 2. Projections Scheme

- Associativity: adding planes sequentially is equivalent to the same procedure developed in just one step;
- Invariance: adding planes which are already in the set does not change the constitutive tensor;
- Idempotence: one obtains a zero populated matrix if the projections are applied to a remainder constitutive tensor of the same decomposition.

By the associative and invariant property, one can define an extraction from an anisotropic tensor to an isotropic one as

$$\mathbf{P}^{(\mathrm{iso})}_{(\mathrm{ful})} = \begin{bmatrix} \frac{1}{2} & 0 & 0 & 0 & 0 & \frac{1}{2} & 0 & 0 & 0 & 0 & 0 & 0 & 0 & 0 & 0 \\ 0 & 1 & 0 & 0 & 0 & 0 & 0 & 0 & 0 & 0 & 0 & 0 & 0 & 0 & 0 \\ 0 & 0 & 0 & 0 & 0 & 0 & 0 & 0 & 0 & 0 & 0 & 0 & 0 & 0 & 0 \\ 0 & 0 & 0 & 0 & 0 & 0 & 0 & 0 & 0 & 0 & 0 & 0 & 0 & 0 & 0 \\ 0 & 0 & 0 & 0 & 0 & 0 & 0 & 0 & 0 & 0 & 0 & 0 & 0 & 0 & 0 \\ \frac{1}{2} & 0 & 0 & 0 & 0 & \frac{1}{2} & 0 & 0 & 0 & 0 & 0 & 0 & 0 & 0 & 0 \\ 0 & 0 & 0 & 0 & 0 & 0 & 0 & 0 & 0 & 0 & 0 & 0 & 0 & 0 & 0 \\ 0 & 0 & 0 & 0 & 0 & 0 & 0 & 0 & 0 & 0 & 0 & 0 & 0 & 0 & 0 \\ 0 & 0 & 0 & 0 & 0 & 0 & 0 & 0 & 0 & 0 & 0 & 0 & 0 & 0 & 0 \\ \frac{1}{4} & -\frac{1}{2} & 0 & 0 & 0 & \frac{1}{4} & 0 & 0 & 0 & 0 & 0 & 0 & 0 & 0 & 0 \\ 0 & 0 & 0 & 0 & 0 & 0 & 0 & 0 & 0 & 0 & 0 & 0 & 0 & 0 & 0 \\ \frac{1}{4} & -\frac{1}{2} & 0 & 0 & 0 & \frac{1}{4} & 0 & 0 & 0 & 0 & 0 & 0 & 0 & 0 & 0 \\ 0 & 0 & 0 & 0 & 0 & 0 & 0 & 0 & 0 & 0 & 0 & 0 & 0 & 0 & 0 \\ \frac{1}{4} & -\frac{1}{2} & 0 & 0 & 0 & \frac{1}{4} & 0 & 0 & 0 & 0 & 0 & 0 & 0 & 0 & 0 \end{bmatrix},$$

in which is essentially the result of the projections of an isotropic symmetry on an anisotropic one, independently of its position in the constitutive hierarchy.

The additive decomposition is then described as

$$\hat{\mathbf{C}} = \hat{\mathbf{C}}^{(\mathrm{iso})} + \hat{\mathbf{C}}^{(\mathrm{ani})}, \tag{7}$$

where

$$\hat{\mathbf{C}}^{(\mathrm{iso})} = \mathrm{vech}^{-1}\left(\mathbf{y}^{(\mathrm{iso})}\right)$$

As aforementioned, $\hat{\mathbf{C}}^{(\mathrm{ani})}$ normally keeps the anisotropic terms of the original tensor. Moreover, despite the positive-definiteness of the original and isotropic constitutive tensors, this property cannot be proved in the remainder tensor.

2.3 *pb-2* Rayleigh-Ritz Method

The degrees-of-freedom are defined by a inner-product between the interpolation functions and the weighting constants vector as

$$\mathbf{d} \doteq \boldsymbol{\Phi}\boldsymbol{\lambda}$$

Table 2. γ_k values for each boundary condition type

		γ_k		
		$g^{(1)}$	$g^{(2)}$	$g^{(3)}$
Clamped	(C)	1	1	1
Simply-Supported	(S)	1	1	0
Free	(F)	0	0	0

where

$$\mathbf{\Phi} = \begin{bmatrix} \boldsymbol{\phi}^{(1)^{\mathrm{T}}} & \mathbf{0} & \mathbf{0} \\ \mathbf{0} & \boldsymbol{\phi}^{(2)^{\mathrm{T}}} & \mathbf{0} \\ \mathbf{0} & \mathbf{0} & \boldsymbol{\phi}^{(3)^{\mathrm{T}}} \end{bmatrix}_{3\times 3n}, \qquad \boldsymbol{\lambda} = \begin{Bmatrix} \mathbf{c}^{(1)} \\ \mathbf{c}^{(2)} \\ \mathbf{c}^{(3)} \end{Bmatrix}_{3n},$$

and

$$\mathbf{c}^{(i)^{\mathrm{T}}} = \left\{ c_1^{(i)} \quad c_2^{(i)} \quad c_3^{(i)} \quad \dots \quad c_n^{(i)} \right\}_n,$$

in which $\boldsymbol{\phi}^{(i)}$ denote kinematic admissible functions, vector $\boldsymbol{\lambda}$ groups the constants of the linear combination, defined by $\mathbf{c}^{(i)}$, being i related to the degrees-of-freedom and n the number of weighting constants in each degree-of-freedom, which is close related to the bases enrichment (Lisbôa *et al.* (2017); Lisbôa and Marczak (2017); Liew (1992)). By the *pb-2* variation, the boundary conditions are employed by a product of monomials, $g^{(\mathrm{i})}$, as

$$g^{(\mathrm{i})}\left(x_1, x_2\right) = \prod_{k=1}^{4} \left[\Theta_k\left(x_1, x_2\right)\right]^{\gamma_k},$$

in which Θ_k are the line equations of the boundary. Being the plate rectangular, these lines are defined as

$$\Theta_1 = x_2, \qquad \Theta_2 = x_1 - a, \qquad \Theta_3 = x_2 - b, \qquad \Theta_4 = x_1,$$

where the plate domain is described by $[0, a] \times [0, b]$. They are applied to the interpolation basis as follows

$$\boldsymbol{\phi}^{(\mathrm{i})}\left(x_1, x_2\right) = g^{(\mathrm{i})}\left(x_1, x_2\right) \boldsymbol{\omega}\left(x_1, x_2\right), \tag{8}$$

in which the $\boldsymbol{\omega}\left(x_1, x_2\right)$ is a vector containing the interpolation functions (not necessarily kinematically admissible). The construction of $\boldsymbol{\phi}^{(i)}\left(x_1, x_2\right)$ follows the procedure presented by Liew (Liew (1992)), which is, basically, a dyadic product between the monomial power sequence in x_1 and x_2), when polynomials are used to interpolate the solution.

For FSDT, γ_k can be either 0 (null) or 1 (one) and, in considering the boundary conditions of Tab. (1), these values are shown in Tab. 2. The letters between parenthesis are symbols that from now on represents the boundary condition type. It is worth to observe that, in simply-supported, the restricted rotation concerns the one in normal direction. Consequently, the values of $g^{(2)}$ and $g^{(3)}$ can be exchanged.

A mapping is produced in order to ease the quadrature process (Gaussian Quadrature) and it is exactly the same as the finite element of four nodes (Reddy (2007)). Due to the plate's geometry, the Jacobian, $|\mathbf{J}|$, depends only on the plate's size. Hence, with the displacement interpolation and the mapping defined, one can determine the strain energy, Eq. (4), and the external potential, Eq. (6), as functions of $\boldsymbol{\lambda}$ as

$$W_{\mathrm{int}} = \frac{1}{2}\boldsymbol{\lambda}^{\mathrm{T}} \int_{-1}^{1}\int_{-1}^{1} \mathbf{\Phi}^{\mathrm{T}}\boldsymbol{\partial}^{\mathrm{T}}\mathbf{T}\boldsymbol{\partial}\mathbf{\Phi}\, |\mathbf{J}|\, \mathrm{d}s_1\mathrm{d}s_2\, \boldsymbol{\lambda} = \frac{1}{2}\boldsymbol{\lambda}^{\mathrm{T}} \int_{-1}^{1}\int_{-1}^{1} \mathbf{B}^{\mathrm{T}}\mathbf{T}\mathbf{B}\, |\mathbf{J}|\, \mathrm{d}s_1\mathrm{d}s_2\, \boldsymbol{\lambda}, \tag{9}$$

$$W_{\mathrm{ext}} = -\int_{-1}^{1}\int_{-1}^{1} \mathbf{q}^{\mathrm{T}}\mathbf{\Phi}\, |\mathbf{J}|\, \mathrm{d}s_1\mathrm{d}s_2\, \boldsymbol{\lambda}. \tag{10}$$

The Total Energy Potential, W_{tot}, is determinate by the sum of the strain energy and external potential (Eqs. (9) and (10)). Thus, its first variation can be determinate by the first partial derivative regarding the vector $\boldsymbol{\lambda}$, as

$$\delta\left(W_{\mathrm{tot}}\right) = \delta\left(W_{\mathrm{int}} - W_{\mathrm{ext}}\right) = 0, \qquad \frac{\partial W_{\mathrm{tot}}}{\partial \boldsymbol{\lambda}} = 0, \qquad \frac{\partial W_{\mathrm{int}}}{\partial \boldsymbol{\lambda}} + \frac{\partial W_{\mathrm{ext}}}{\partial \boldsymbol{\lambda}} = \mathbf{0}.$$

The strain energy variation is then determined as

$$W_{\mathrm{int}} = \int_{-1}^{1}\int_{-1}^{1} \mathbf{B}^{\mathrm{T}}\mathbf{T}\mathbf{B}\, |\mathbf{J}|\, \mathrm{d}s_1\mathrm{d}s_2\, \boldsymbol{\lambda} = \mathbf{N}\boldsymbol{\lambda}.$$

In a similar fashion, the external potential expressed in the Eq. (10) is calculated as

$$\frac{\partial \mathrm{W}_{\mathrm{ext}}}{\partial \boldsymbol{\lambda}} = -\int_{-1}^{1}\int_{-1}^{1} \boldsymbol{\Phi}^{\mathrm{T}}\mathbf{q}\,|\mathbf{J}|\,\mathrm{d}s_1\mathrm{d}s_2 = -\mathbf{v},$$

resulting in

$$\mathbf{N}\boldsymbol{\lambda} = \mathbf{v}. \tag{11}$$

The linear system in the Eq. (11) is solved in a recursive fashion by the Adomian Decomposition Method.

3. ADOMIAN DECOMPOSITION METHOD

In considering a differential matrix linear operator $\mathcal{L}(\boldsymbol{\partial}_{\mathbf{x}})$ which resembles the thick plate differential operator, a vectorial function $\mathbf{u}$ and an external excitation $\mathbf{f}$, the boundary value problem can written as

$$\mathcal{L}(\boldsymbol{\partial}_{\mathbf{x}})\mathbf{u}(\mathbf{x}) = \mathbf{f}. \tag{12}$$

Equation (12) is subject to a set of boundary conditions (Tab. (1)). The operator is decomposed into two by some predefined rule, as well as the $\mathbf{u}(\mathbf{x})$ is expanded in an infinite series. Therefore, one redefines Eq. (12) as

$$\left[\mathcal{L}^{(1)}(\boldsymbol{\partial}_{\mathbf{x}}) + \mathcal{L}^{(2)}(\boldsymbol{\partial}_{\mathbf{x}})\right]\left[\mathbf{u}^{(0)}(\mathbf{x}) + \mathbf{u}^{(1)}(\mathbf{x}) + \cdots + \mathbf{u}^{(k)}(\mathbf{x}) + \cdots\right] = \mathbf{f}, \tag{13}$$

which is recursively solved as

$$\begin{aligned}
&\mathcal{L}^{(1)}(\boldsymbol{\partial}_{\mathbf{x}})\mathbf{u}^{(0)}(\mathbf{x}) = \mathbf{f},\\
&\mathcal{L}^{(1)}(\boldsymbol{\partial}_{\mathbf{x}})\mathbf{u}^{(1)}(\mathbf{x}) = -\mathcal{L}^{(2)}(\boldsymbol{\partial}_{\mathbf{x}})\mathbf{u}^{(0)}(\mathbf{x}),\\
&\mathcal{L}^{(1)}(\boldsymbol{\partial}_{\mathbf{x}})\mathbf{u}^{(2)}(\mathbf{x}) = -\mathcal{L}^{(2)}(\boldsymbol{\partial}_{\mathbf{x}})\mathbf{u}^{(1)}(\mathbf{x}),\\
&\qquad\qquad\vdots\\
&\mathcal{L}^{(1)}(\boldsymbol{\partial}_{\mathbf{x}})\mathbf{u}^{(k)}(\mathbf{x}) = -\mathcal{L}^{(2)}(\boldsymbol{\partial}_{\mathbf{x}})\mathbf{u}^{(k-1)}(\mathbf{x}).
\end{aligned} \tag{14}$$

The recursive system of Eq. (14) is interesting in a physical view, if the operator superposition has some physical meaning. In the formulation presented herein, the decomposition is governed by a hierarchy of constitutive symmetries (Fig. 1). In considering the irreducible symmetry (isotropic) the recursive system of Eq. (14) clearly describes an enhancement of an isotropic solution by anisotropic terms. This statement is imperative due to the fact that for several physical problems, isotropic solutions are readily available while its anisotropic counterpart are not. Moreover, as one notices, from the second equation of Eq. (14), only the particular solution is required, since the homogeneous one is determined in the first equation and it is part of the isotropic response.

Equation (12) can be translated to the linear system of Eq. (11). Therefore, the decomposition in eq. (7) is applied to the stiffness matrix (Eq. (5)), resulting in

$$\mathbf{T} = \mathbf{T}^{(\mathrm{iso})} + \mathbf{T}^{(\mathrm{ani})} \quad \Rightarrow \quad \mathbf{N} = \mathbf{N}^{(\mathrm{iso})} + \mathbf{N}^{(\mathrm{ani})}. \tag{15}$$

The expansion of the plate's displacement can be related to the same procedure applied to the constants vector $\boldsymbol{\lambda}$. So

$$\begin{aligned}
\mathbf{d} &= \mathbf{d}^{(0)} + \mathbf{d}^{(1)} + \mathbf{d}^{(2)} + \ldots + \mathbf{d}^{(k)} + \ldots\\
&= \boldsymbol{\Phi}\boldsymbol{\lambda}^{(0)} + \boldsymbol{\Phi}\boldsymbol{\lambda}^{(1)} + \boldsymbol{\Phi}\boldsymbol{\lambda}^{(2)} + \ldots + \boldsymbol{\Phi}\boldsymbol{\lambda}^{(k)} + \ldots\\
\mathbf{d} &= \boldsymbol{\Phi}\left(\boldsymbol{\lambda}^{(0)} + \boldsymbol{\lambda}^{(1)} + \boldsymbol{\lambda}^{(2)} + \ldots + \boldsymbol{\lambda}^{(k)} + \ldots\right) = \boldsymbol{\Phi}\boldsymbol{\lambda},
\end{aligned} \tag{16}$$

resulting in

$$\boldsymbol{\lambda} = \boldsymbol{\lambda}^{(0)} + \boldsymbol{\lambda}^{(1)} + \boldsymbol{\lambda}^{(2)} + \ldots + \boldsymbol{\lambda}^{(k)} + \ldots, \tag{17}$$

in which is considered that each term of the expanded solution has the same interpolation basis (Eq. (16)). This hypothesis simplifies the analysis without losing generality. Equation (17) expresses that using ADM together with RRM, the expansion of the solution is equivalent to expanding the constants vector $\boldsymbol{\lambda}$. The same conclusion is found in refs. (Lisbôa *et al.* (2017); Lisbôa and Marczak (2017)). In inserting the Eqs. (15)-(17) into Eq. (11) one finds

$$\left(\mathbf{N}^{(\mathrm{iso})} + \mathbf{N}^{(\mathrm{ani})}\right)\left(\boldsymbol{\lambda}^{(0)} + \boldsymbol{\lambda}^{(1)} + \boldsymbol{\lambda}^{(2)} + \ldots + \boldsymbol{\lambda}^{(k)} + \ldots\right) = \mathbf{v},$$

which has the same structure of Eq. (13). Thus

$$\begin{aligned}
\mathbf{N}^{(\mathrm{iso})}\boldsymbol{\lambda}^{(0)} &= \mathbf{v},\\
\mathbf{N}^{(\mathrm{iso})}\boldsymbol{\lambda}^{(1)} &= -\mathbf{N}^{(\mathrm{ani})}\boldsymbol{\lambda}^{(0)},\\
\mathbf{N}^{(\mathrm{iso})}\boldsymbol{\lambda}^{(2)} &= -\mathbf{N}^{(\mathrm{ani})}\boldsymbol{\lambda}^{(1)},\\
&\vdots\\
\mathbf{N}^{(\mathrm{iso})}\boldsymbol{\lambda}^{(k)} &= -\mathbf{N}^{(\mathrm{ani})}\boldsymbol{\lambda}^{(k-1)},\\
&\vdots
\end{aligned}$$

By solving these equation, one can construct the full response of an anisotropic plate which the first step of the recursive system is the isotropic solution of the same differential equation, boundary and loading conditions.

The stopping criteria of the recursive methodology is defined as a achieved tolerance, determined from two sequential approximations. The normalised distances is then derived as

$$\begin{aligned}
e_{u_3} &= \frac{\left\langle u_3^{(m+1)} - u_3^{(m)} | u_3^{(m+1)} - u_3^{(m)} \right\rangle}{\left\langle u_3^{(m)} | u_3^{(m)} \right\rangle},\\
e_{\theta_1} &= \frac{\left\langle \theta_1^{(m+1)} - \theta_1^{(m)} | \theta_1^{(m+1)} - \theta_1^{(m)} \right\rangle}{\left\langle \theta_1^{(m)} | \theta_1^{(m)} \right\rangle},\\
e_{\theta_2} &= \frac{\left\langle \theta_2^{(m+1)} - \theta_2^{(m)} | \theta_2^{(m+1)} - \theta_2^{(m)} \right\rangle}{\left\langle \theta_2^{(m)} | \theta_2^{(m)} \right\rangle},
\end{aligned} \tag{18}$$

where m corresponds to the previous step and $\langle\cdot|\cdot\rangle$ to the inner-product, which is carried out by L^2 norm. After some algebraic manipulations, Eqs. (18) are rewritten as one by

$$e^{(m+1)} = \left[\frac{\boldsymbol{\lambda}^{(m+1)^{\mathrm{T}}} \int_\Lambda \boldsymbol{\Phi}^{\mathrm{T}}\boldsymbol{\Phi}\, \mathrm{d}\Lambda \boldsymbol{\lambda}^{(m+1)}}{\left(\sum_{n=0}^{m} \boldsymbol{\lambda}^{(m)^{\mathrm{T}}}\right) \int_\Lambda \boldsymbol{\Phi}^{\mathrm{T}}\boldsymbol{\Phi}\, \mathrm{d}\Lambda \left(\sum_{n=0}^{m} \boldsymbol{\lambda}^{(m)}\right)} \right]^{\frac{1}{2}} \tag{19}$$

One notices that the denominator of Eq. (19) is the inner-product the displacement field of the previous step while the nominator is the added term in the $m+1$ step. The ratio defines how much the step changes the solution in a normalized fashion. Values of $e^{(m)}$ are related to a numeric tolerance in order to be a parameter for the stopping criteria.

4. NUMERIC RESULTS

A numeric routine based on the presented methodology is developed in order to verify the problem's convergence and to compare the obtained solutions with those found in the literature. There are two convergences regarding the methodology: the RRM and the ADM ones. Both are analysed in this section. Then, parameters such as material, thickness and plate's size are varied and their solutions under uniform loading are provided by this methodology. All results are compared with numeric results obtained by the Finite Element Method using a commercial software Ansys ® Inc. (2017) and/or by results found in the literature.

The material used in all numeric analysis is set as (Lisbôa *et al.* (2017); Ting and Kim (2012))

$$E_{11} = \alpha E_{22}, \qquad G_{12} = 0.6E_{22}, \qquad G_{13} = 0.5E_{22}, \qquad G_{23} = 0.6E_{22}, \qquad \nu_{12} = 0.25,$$

which belongs to an orthorhombic symmetry. The constitutive properties are related to the elastic modulus, for the reduced constitutive tensor (eq. (2)), as

$$\begin{aligned}
\hat{C}_{11} &= \frac{E_{11}}{1-\nu_{12}\nu_{21}}, & \hat{C}_{22} &= \frac{E_{22}}{1-\nu_{12}\nu_{21}}, & \hat{C}_{12} &= \frac{E_{22}\nu_{21}}{1-\nu_{12}\nu_{21}},\\
\hat{C}_{44} &= G_{23}, & \hat{C}_{55} &= G_{13}, & \hat{C}_{66} &= G_{12},
\end{aligned}$$

and $\nu_{12}E_{22} = \nu_{21}E_{11}$.

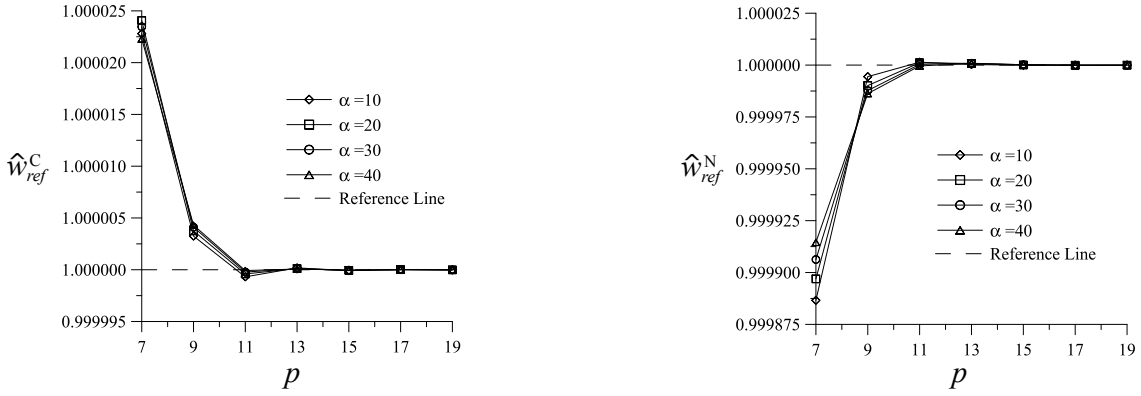

Figure 3. RRM convergence of square FSFS with $a/h = 5$ at (a) plate's center and (b) free edge center.

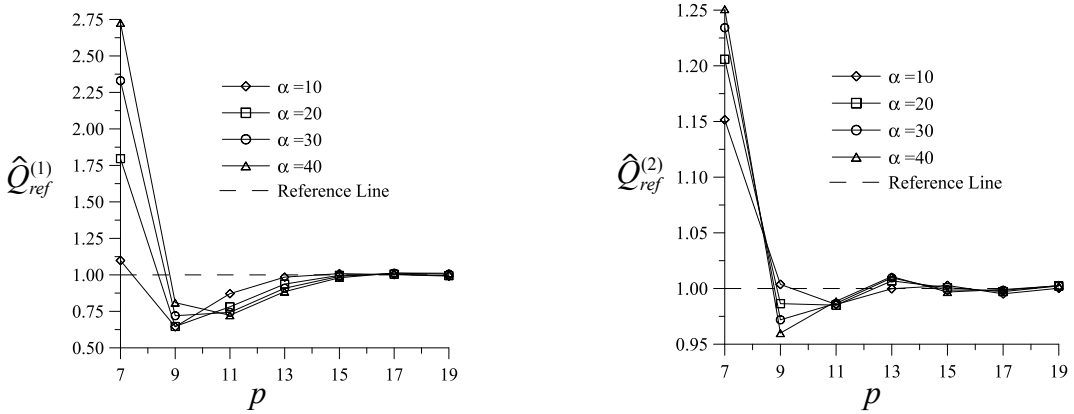

Figure 4. RRM convergence of transverse shear of rectangular CCCS plates with $a/h = 100$: (c) S_{13} and (d) S_{23}.

In order to present the obtained results, both in convergence studies and in numeric tables, some variables are made non-dimensional as follow (Ting and Kim (2012))

$$\hat{w}^{\mathrm{pos}} = \frac{100u_3(x_1^{\mathrm{pos}}, x_2^{\mathrm{pos}})E_2h^3}{q_3a^4}, \qquad \hat{M}^{\mathrm{pos}}_{\alpha\beta} = \frac{M_{\alpha\beta}(x_1^{\mathrm{pos}}, x_2^{\mathrm{pos}})}{q_3a^2}, \qquad \hat{S}_{\alpha 3} = \frac{S_{\alpha 3}(x_1^{\mathrm{pos}}, x_2^{\mathrm{pos}})}{2q_3a},$$

and

$$\hat{w}^{\mathrm{pos}}_{ref} = \frac{\hat{w}^{\mathrm{pos}}}{\hat{w}^{c}_{ref}}, \qquad \hat{w}^{\mathrm{conv}} = \frac{\hat{w}_{n_{int}}}{\hat{w}^{c}_{ref}}, \qquad \hat{M}^{(\alpha\beta)}_{ref} = \frac{\hat{M}_{\alpha\beta}}{\hat{M}^{c}_{ref}}, \qquad \hat{Q}^{(\alpha)}_{ref} = \frac{\hat{S}_{\alpha 3}}{\hat{S}^{c}_{ref}},$$

noticing that $(\hat{\cdot})$ and $(\cdot)_{ref}$ denote non-dimensional variables, converged and reference (converged) values, respectively. pos corresponds to the assessed position as $\mathrm{pos} = \{\mathrm{C}, \mathrm{N}, \mathrm{S}, \mathrm{E}, \mathrm{W}, \mathrm{NE}\}$ and are related to the cardinal directions taken from C (plate's centre). n_{int} denotes the number of an iteration while $\hat{w}^{\mathrm{conv}}$ presentes the ratio between the iteration centre displacement and the converged one. $\hat{Q}^{(\alpha)}_{ref}$ and $\hat{M}^{(\alpha\beta)}_{ref}$ are assessed in the same position for all analysis: $\hat{Q}^{(1)}_{ref}$ in $\mathrm{pos} = \mathrm{E}$, $\hat{Q}^{(2)}_{ref}$ in $\mathrm{pos} = \mathrm{N}$ and $\hat{M}^{(\alpha\beta)}_{ref}$ in $\mathrm{pos} = \mathrm{C}$.

Numeric results obtained by FEM are developed using a 8-node shell element Ansys ® Inc. (2017) based on Mindlin plate theory (SHELL181). A mesh of 80 elements per metre is considered. Being the plate rectangular, the boundary condition sets are described by four upper-case letters, regarding Tab. (1), starting from the south edge and turning into the right-hand direction.

The method convergence regarding the RRM is tested and presented in Tab. 3 as well as depicted in the Figs. 3-4, in which the reference line depicts the converged value and p denotes the highest polynomial degree of $\boldsymbol{\omega}$ (Eq. (8)). Table 3 presents the convergence of the transverse displacement, bending moments and transverse shear for a square SSSS plates with $\alpha = 10$ and $a/h = 10$. As expected the displacement convergence is relatively fast when comparing to the other parameters in analysis. The transverse shear convergence shows that 4-digits may be predicted by RRM with $p = 19$, in spite of recognizing that this parameter has a slower convergence. Figure 3 depicts the convergence of square FSFS plates with $a/h = 50$. It shows that α has little influence on the displacement convergence. Figure 4 presents the convergence for S_{13} and S_{23} for rectangular CCCS plates with $a/h = 100$.

Table 3. Convergence for square SSSS plates with $\alpha = 10$ and $a/h = 10$ under uniform loading

p	n_I	$\hat{w}^C$	M_{11}^C	M_{22}^C	$\hat{S}_{23}^N$	$\hat{S}_{13}^E$
5	92	1.5847604	0.1097744	0.012290728	-0.096497854	-0.240606151
7	92	1.5852111	0.110115997	0.012407693	-0.091771007	-0.241941752
9	92	1.5852024	0.110051088	0.012363607	-0.092410716	-0.244570562
11	92	1.5851584	0.110070003	0.012377924	-0.093330134	-0.244005033
13	92	1.5851887	0.110061918	0.012371797	-0.093210467	-0.243571118
15	92	1.5851690	0.110065548	0.012374588	-0.093038126	-0.243718679
17	92	1.5851815	0.110063649	0.012373198	-0.093060369	-0.243786467
19	92	1.5851734	0.110064687	0.012373948	-0.093090582	-0.243754079
Ansys ® Inc. (2017)	-	1.5851797	0.11006291	0.012373646	-0.092460115	-0.243125570

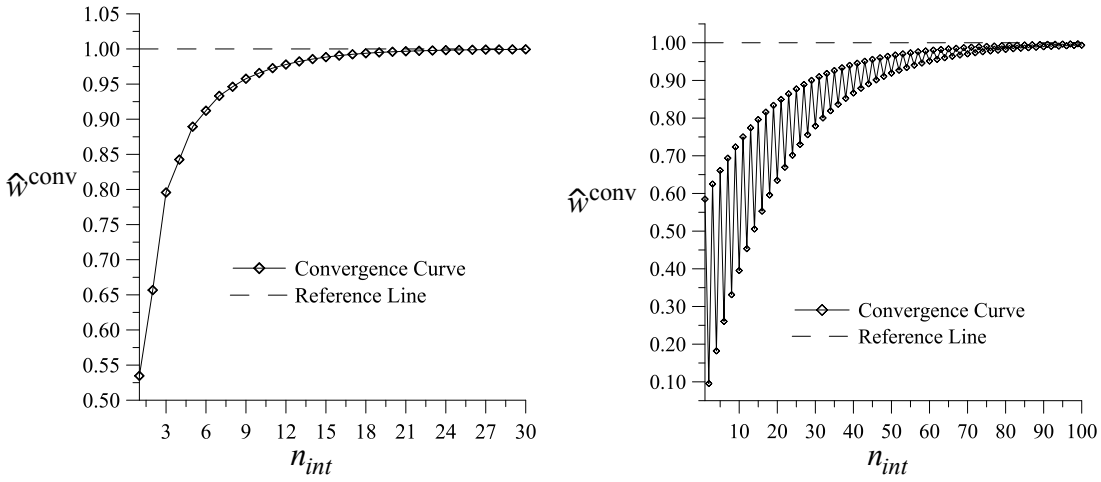

Figure 5. Convergence of ADM for: (a) square CFFC plate and (b) square FSFS plate

The convergence can be easily observed in both Tab. 3 and Figs. 3 and 4 having however a small difference with FEM results. An error measurement is defined as the relative error between the present solution and those produced by FEM. In Tab. 3, for all variables, this error was smaller than 1%. This corresponds to a small discrepancy in the third significant digit. Mostly, such high errors were found in transverse shear comparisons, being this an expected behaviour: given the relationship between the interpolated variables (displacements) and the transverse shear, the convergence rate might be (and it was) lower than the displacement and rotations.

Figure 5 presents the convergence behaviour of ADM for two boundary conditions: CSSC and FSFS. As one notes, their form is similar: monotonically increasing, in a mean sense. For all cases herein analysed, the tolerance for the stopping criterion was set as 10^{-10}. Consequently, the number of iterations was high for all studied cases. In most of analysed cases, the convergence is similar to square CSSC convergence (Figure 5). It is important to observe that the first iteration of the recursive procedure concerns to an isotropic response. As presented in Fig. 5, these solutions could be far, in a L^2 sense, to the converged one. In the CSSC and FSFS plates, the centre transverse displacement is $\approx 60\%$ of the anisotropic one.

Due to the good agreement between the reference solutions and those herein presented, two boundary conditions sets, plate's thickness and size as well as constitutive properties was varied in order to provide numeric results. For each case of study, numeric values of centre transverse displacement, bending moments, transverse shear are provided. In each analysis, a convergence study, which was identical to the Tab. 3, was carried out in order to determine properly the significant digits of all assessed variables. The Tab. 4 are subdivided into four vertical and two horizontal groups, regarding the material and the plate's size, respectively. In each division, a maximum relative error of the assessed variables are provided so as to evaluate the precision of the numeric results with respect to FEM analysis. These two tables are produced in order to demonstrate the potential of the methodology. These tables could be improved by considering other parameters as well as other boundary conditions.

5. CONCLUSIONS

Adomian Decomposition Method along with *pb-2* Rayleigh-Ritz Method were applied to Mindlin's plate theory in order to analyse properties of the first method when applied to partial elliptic differential equations. The decomposition method requires the decomposition of the differential/matrix operator. The paper's proposition was to use a constitutive

Table 4. Transverse displacement, bending moments and transverse shear for rectangular and square SSSS plates

		$a/b = 1/2$						$a/b = 1$					
α	$\frac{a}{h}$	n_I	$\hat{w}^{\mathrm{C}}$	$\hat{M}_{11}^{\mathrm{C}}$	$\hat{M}_{22}^{\mathrm{C}}$	$\hat{Q}_{23}^{\mathrm{N}}$	$\hat{Q}_{13}^{\mathrm{E}}$	n_I	$\hat{w}^{\mathrm{C}}$	$\hat{M}_{11}^{\mathrm{C}}$	$\hat{M}_{22}^{\mathrm{C}}$	$\hat{Q}_{23}^{\mathrm{N}}$	$\hat{Q}_{13}^{\mathrm{E}}$
10	5	96	2.6018	0.127248	0.003961	-0.0960	-0.25475	98	2.20346	0.104472	0.015375	-0.09945	-0.238
	10	92	1.83201	0.127095	0.003470	-0.0909	-0.25385	92	1.58518	0.110064	0.012374	-0.09305	-0.24375
	50	76	1.585741	0.126934	0.003353	-0.0895	-0.2535	75	1.3801487	0.112031	0.0112693	-0.09095	-0.2457
	100	68	1.578049	0.126928	0.003350	-0.0895	-0.2535	70	1.373676	0.112093	0.0112336	-0.0910	-0.246
e_{max}		-	0.00	0.00	0.02	1.91	0.55	-	0.00	0.00	0.00	0.76	0.41
20	5	195	1.8185	0.127815	0.001623	-0.0828	-0.25445	195	1.71989	0.117070	0.010985	-0.084865	-0.251
	10	188	1.04204	0.126656	0.001380	-0.0746	-0.25225	186	1.02677	0.124328	0.006935	-0.075085	-0.258
	50	159	0.795889	0.126110	0.001394	-0.0715	-0.2515	159	0.792602	0.126521	0.0054661	-0.07175	-0.260
	100	144	0.788226	0.126092	0.001395	-0.0715	-0.251	148	0.7851758	0.126582	0.0054196	-0.0715	-0.260
e_{max}		-	0.00	0.00	0.03	1.87	0.54	-	0.00	0.00	0.00	0.92	0.38
30	5	292	1.5505	0.127630	0.000906	-0.0775	-0.25395	291	1.52704	0.121835	0.009251	-0.07892	-0.2559
	10	283	0.77554	0.125995	0.000823	-0.06745	-0.2512	280	0.79977	0.129337	0.004787	-0.067315	-0.26275
	50	241	0.531418	0.125373	0.000904	-0.063	-0.250	241	0.5525711	0.131010	0.0032250	-0.0631	-0.2635
	100	221	0.523832	0.12536	0.000907	-0.063	-0.250	225	0.5447303	0.131040	0.0031774	-0.063	-0.2635
e_{max}		-	0.00	0.01	0.06	2.05	0.51	-	0.00	0.00	0.01	1.16	0.28
40	5	388	1.4157	0.127444	0.000568	-0.0746	-0.25355	386	1.4234	0.124304	0.008324	-0.07568	-0.2584
	10	377	0.6427	0.125581	0.000582	-0.0632	-0.2506	373	0.67695	0.131665	0.003654	-0.06288	-0.26485
	50	323	0.400122	0.125015	0.000692	-0.058	-0.2495	322	0.4228258	0.132593	0.0020878	-0.0579	-0.2645
	100	296	0.392587	0.12500	0.000696	-0.0575	-0.2495	300	0.4147793	0.132581	0.0020423	-0.058	-0.2645
e_{max}		-	0.00	0.01	0.09	2.13	0.50	-	0.00	0.00	0.01	1.70	0.36

Table 5. Transverse displacement, bending moments and transverse shear for rectangular and square SSCC plates

		$a/b = 1/2$						$a/b = 1$					
α	$\frac{a}{h}$	n_I	$\hat{w}^{\mathrm{C}}$	$\hat{M}_{11}^{\mathrm{C}}$	$\hat{M}_{22}^{\mathrm{C}}$	$\hat{Q}_{23}^{\mathrm{N}}$	$\hat{Q}_{13}^{\mathrm{E}}$	n_I	$\hat{w}^{\mathrm{C}}$	$\hat{M}_{11}^{\mathrm{C}}$	$\hat{M}_{22}^{\mathrm{C}}$	$\hat{Q}_{23}^{\mathrm{N}}$	$\hat{Q}_{13}^{\mathrm{E}}$
10	5	98	1.81502	0.07450	0.002279	-0.1397	-0.2016	101	1.55770	0.06191	0.011411	-0.14297	-0.18995
	10	95	0.928032	0.06641	0.001573	-0.13355	-0.1924	95	0.858679	0.06127	0.007314	-0.135	-0.19005
	50	80	0.63856	0.063179	0.001473	-0.1345	-0.189	82	0.605006	0.060635	0.005502	-0.1349	-0.1895
	100	76	0.629482	0.063073	0.001471	-0.135	-0.189	77	0.596733	0.060604	0.005441	-0.13535	-0.190
e_{max}		-	0.01	0.51	0.69	1.36	0.89	-	0.00	0.18	0.19	0.48	0.51
20	5	197	1.4756	0.08210	0.001115	-0.1278	-0.20875	201	1.35038	0.07268	0.009277	-0.1304	-0.20215
	10	193	0.60817	0.06869	0.000691	-0.1147	-0.19405	192	0.61144	0.06874	0.004437	-0.115	-0.1994
	50	168	0.32372	0.062802	0.000716	-0.10915	-0.188	169	0.3336884	0.065157	0.002327	-0.10855	-0.196
	100	152	0.314777	0.062605	0.000717	-0.1095	-0.1875	158	0.324554	0.064990	0.0022612	-0.10865	-0.196
e_{max}		-	0.01	0.51	0.69	1.95	0.80	-	0.00	0.21	0.34	0.63	0.58
30	5	294	1.3513	0.08772	0.000722	-0.12305	-0.21415	298	1.26691	0.07952	0.008428	-0.12532	-0.20945
	10	289	0.5004	0.07094	0.000441	-0.1069	-0.19605	287	0.51644	0.07290	0.003365	-0.10685	-0.204
	50	256	0.21956	0.062807	0.000497	-0.097	-0.1875	255	0.2301884	0.066123	0.001242	-0.09645	-0.1965
	100	234	0.21067	0.062525	0.000498	-0.097	-0.1875	238	0.2207572	0.065800	0.0011826	-0.0965	-0.1965
e_{max}		-	0.01	0.51	0.74	1.93	0.73	-	0.00	0.23	0.50	0.90	0.58
40	5	389	1.2841	0.09208	0.000519	-0.1204	-0.2184	394	1.21991	0.08457	0.007955	-0.12245	-0.21465
	10	384	0.44589	0.07309	0.000324	-0.1025	-0.1981	380	0.46574	0.07603	0.002805	-0.1023	-0.20725
	50	342	0.16767	0.062918	0.000386	-0.0895	-0.1875	342	0.1760649	0.066268	0.000739	-0.08905	-0.196
	100	314	0.158795	0.062549	0.000385	-0.089	-0.1875	317	0.1665294	0.065789	0.0006883	-0.089	-0.1955
e_{max}		-	0.01	0.51	0.81	1.81	0.70	-	0.00	0.24	0.70	1.12	0.39

decomposition governed by a constitutive hierarchy. A constitutive hierarchy was devised to the symmetries of the reduced constitutive tensor as well as projections were developed so as to extract lower constitutive symmetries from higher ones. The recursive methodology was presented and its convergence was shown numerically and presented different behaviours depending on the boundary conditions set. Due to the good agreement between the obtained solutions and those derived by FEM, two tables with numeric results were developed.

Regarding the methodology, it is proved that it can be used to derive anisotropic responses of thick plates. In spite of the number of iterations appearing to be high, the numeric procedure is fast (matrix-vector product), turning the methodology a real alternative to be applied in anisotropic problems. Moreover, in order to achieve benchmark solutions for bending moments and transverse shear stress, the tolerance was set very low ($10^{(-10)}$). This value can can be certainly increased with small loss of precision but with a significant decline in the number of iterations, given the Adomian Decomposition Method convergence characteristics.

The results of this paper can work as base for future works in physical phenomena in which the degree of anisotropy changes during the deformation process as well as optimisation problems where the the elastic properties are the design variable.

6. ACKNOWLEDGEMENTS

Marczak and Lisbôa would like to acknowledge CAPES (Coordination for the Improvement of Higher Educational Personnel) and CNPq (National Council for Scientific and Technological Development) for funding the research project.

7. REFERENCES

Adomian, G., 1994. *Solving Frontier Problems of Physics: The Decomposition Method*. Kluwer Academic Publishers, Dordrecht. ISBN 978-90-481-4352-8.

Alternbach, H., 1998. "Theories for laminated and sandwich plates". *Mechanics of Composite Materials*, Vol. 34, No. 3, pp. 243–252. doi:10.1007/BF02256043.

Ansys ® Inc., 2017. *User Guide*. Ansys ® Inc.

Babolian, E. and Biazar, J., 2002. "Solution of nonlinear equations by modified adomian decomposition method". *Applied Mathematics and Computation*, Vol. 132, No. 1, pp. 167–172. doi:10.1016/S0096-3003(01)00184-9.

Bhat, R.B., 1985. "Plate deflections using orthogonal polynomials". *Journal of Engineering Mechanics*, Vol. 111, No. 11, pp. 1301–1309. doi:10.1061/(ASCE)0733-9399(1985)111:11(1301).

Biazar, J., Babolian, E. and Islam, R., 2004. "Solution of the system of ordinary differential equations by adomian decomposition method". *Applied Mathematics and Computation*, Vol. 147, No. 3, pp. 713–719. doi:10.1016/S0096-3003(02)00806-8.

Browaeys, J.T. and Chevrot, S., 2004. "Decomposition fo the elastic tensor and geophysical applications". *Geophysical Journal International*, Vol. 159, No. 2, pp. 667–678. doi:10.1111/j.1365-246X.2004.02415.x.

Chadwick, P., Vianello, M. and Cowin, S.C., 2001. "A new proof that the number of linear elastic symmetries is eight". *Journal of the Mechanics and Physics of Solids*, Vol. 49, No. 11, pp. 2471–2492. doi:10.1016/S0022-5096(01)00064-3.

Cowin, S.C. and Mehrabadi, M.M., 1995. "Anisotropic symmetries of linear elasticity". *Applied Mechanics Reviews*, Vol. 48, No. 5, pp. 247–285. doi:10.1115/1.3005102.

Haggblad, B. and Bathe, K.J., 1990. "Specifications of boundary conditions for reissner/mindlin plate bending finite elements". *International Journal for Numerical Method in Engineering*, Vol. 30, No. 5, pp. 9981–1011.

Jemielita, G., 2002. "Symmetry classes for elasticity tensors". *Journal of Theoretical and Applied Mechanics*, Vol. 40, No. 1, pp. 73–84.

Kitipornchai, S., Xiang, Y., Liew, K.M. and Lim, M.K., 1994. "A global approach for vibration of thick trapezoidal plates". *Computers & Structures*, Vol. 53, No. 1, pp. 83–92. doi:10.1016/0045-7949(94)90132-5.

Liew, K.M., 1992. "Response of plates of arbitrary shape subject to static loading". *Journal of Engineering Mechanics*, Vol. 118, No. 9, pp. 1783–1794. doi:10.1061/(ASCE)0733-9399(1992)118:9(1783).

Liew, K.M. and Wang, C.M., 1993. "*Pb-2* rayleigh-ritz method for general plate analysis". *Engineering Structures*, Vol. 15, No. 1, pp. 55–60. doi:10.1016/0141-0296(93)90017-X.

Lisbôa, T.V., Geiger, F.P. and Marczak, R.J., 2017. "A recursive methodology to determine the mechanical response of thin laminated plates in bending (accepted for publication)". *Journal of Aerospace Technology and Management*, Vol. 9, No. 4.

Lisbôa, T.V. and Marczak, R.J., 2017. "A recursive methodology for the solution of semi-analytical rectangular anisotropic thin plates in linear bending". *Applied Mathematical Modelling*, Vol. 48, pp. 711–730. doi: 10.1016/j.apm.2017.04.020.

Mindlin, R.D., 1951. "Influence of rotary inertia and shear on flexural motions of elastic plates". *Journal of Applied Mechanics*, Vol. 18, pp. 31–38.

Reddy, J.N., 2004. *Mechanics of Laminated Composite Plates and Shells*. CRC Press, Boca Raton. ISBN 0-8493-1592-1.

Reddy, J.N., 2007. *Theory and Analysis of Elastic Plates and Shells*. CRC Press, Boca Raton. ISBN 978-0-8493-8415-8.

Singh, A.V. and Elaghabash, Y., 2003. "On finite displacement analysis of quadrangular plates". *International Journal of Non-Linear Mechanics*, Vol. 38, No. 8, pp. 1149–1162.

Ting, H.T. and Kim, S.E., 2012. "Analytical solution of a two variable refined plate theory for bending analysis of orthorhombic levy-type plates". *International Journal of Mechanical Sciences*, Vol. 54, No. 1, pp. 269–276. doi: 10.1016/j.ijmecsci.2011.11.007.

Ting, T.C.T., 2003. "Generalized cowin-mehrabadi theorems and a direct proof that the number of linear elastic symmetries is eight". *International Journal of Solids and Structures*, Vol. 40, No. 25, pp. 7129–7142. doi:10.1016/S0020-7683(03)00358-5.

Tu, Y.O., 1968. "The decomposition of an anisotropic elastic tensor". *Acta Crystallographica Section A*, Vol. 24, No. 2, pp. 273–282. doi:10.1107/S0567739468000458.

8. RESPONSIBILITY NOTICE

The authors are the only responsible for the printed material included in this paper.